TRACKING FLUID TEMPERATURE AND δ18O IN CARBONATE-HOSTED HYDROTHERMAL ORE SYSTEMS USING CLUMPED C-O ISOTOPES

Steven P. Hollis,[1,2,†] Paul F. Dennis,[3] Julian F. Menuge,[1] Aileen L. Doran,[1] Alina Marca,[3] Brett Davidheiser-Kroll,[4] Jamie J. Wilkinson,[5,6] Kathryn E. Snell,[4] Oakley Turner,[7] John Güven,[1] and Adrian Boyce[8]

[1]iCRAG (Irish Centre for Research in Applied Geosciences) and School of Earth Sciences, University College Dublin, Belfield, Dublin D04 V1W8, Ireland

[2]School of Geosciences, Grant Institute, James Hutton Road, King's Buildings, University of Edinburgh, Scotland EH9 3FE, United Kingdom

[3]Stable Isotope Laboratory, School of Environmental Sciences, University of East Anglia, Norwich, NR4 7TJ, United Kingdom

[4]Department of Geological Sciences, University of Colorado at Boulder, Boulder, Colorado 80309, United States

[5]London Centre for Ore Deposits and Exploration (LODE), Natural History Museum, Cromwell Road, London SW7 5BD, United Kingdom

[6]Department of Earth Science and Engineering, Imperial College London, Exhibition Road, London SW7 2AZ, United Kingdom

[7]iCRAG (Irish Centre for Research in Applied Geosciences) and Department of Geology, Trinity College Dublin, College Green, Dublin 2, Ireland

[8]Scottish Universities Environmental Research Centre (SUERC), East Kilbride, Glasgow G75 0QF, United Kingdom

Abstract

Carbonates are ubiquitous gangue phases in many hydrothermal ore deposits, often forming throughout the lifetime of individual systems. Clumped C-O isotope analysis represents a novel technique for the acquisition of accurate carbonate precipitation temperatures, allowing calculation of fluid δ18O values. This may be particularly useful when suitable fluid inclusions are not available. We have applied this technique to the Irish Zn-Pb ore field to test the applicability of clumped isotope analysis on a hydrothermal system. We demonstrate a close match between clumped isotope temperatures ($T\Delta_{47}$) and fluid inclusion homogenization temperatures (T_h), particularly in dolomite from Lisheen, and late calcite veins that contain remobilized sphalerite above the South West Extension orebody at Navan. At the Lisheen deposit, our new data confirm that hydrothermal dolomitization at ~150° to 210°C led to the recrystallization and isotopic resetting of earlier, fine-grained diagenetic dolomite. Subsequent carbonate phases were precipitated from hydrothermal fluids in isotopic equilibrium with these early, widespread dolomite phases, as ascending, hot (170°–220°C), mildly acidic fluids produced dissolution (pseudo)breccias and extensive replacement in the Waulsortian limestone. In the hanging wall of the Lisheen deposit, white hydrothermal dolomites formed at ~100° to 170°C, cementing subsidence breccias formed above the orebodies. Calcite in basement veins from Navan yields $T\Delta_{47}$ values ~30° to 40°C lower than measured T_h. This likely reflects either solid-state bond reordering due to burial or skewed T_h distributions due to the failure of bubbles to nucleate in fluid inclusions trapped at low temperatures. Clumped isotope analysis has the potential to revolutionize our understanding of a range of ore systems, particularly when combined with traditional methodologies (e.g., fluid δD, crush-leach) and in situ techniques such as laser ablation-inductively coupled plasma-mass spectrometry (LA-ICP-MS) analysis of minerals and fluid inclusions and U-Pb carbonate geochronology. However, care must be taken with regard to sample characterization, sulfide contamination, and the subsequent burial history of samples.

Introduction

Significant challenges remain in determining the formation temperatures of fossil hydrothermal systems, with fluid inclusion analysis being the most often used technique (Wilkinson, 2001, 2010). There are, however, problems commonly encountered when attempting to determine fluid temperatures from inclusion homogenization temperatures (T_h). Fluid inclusions may be too small, very rare, stretched, or ruptured after formation, and it is frequently difficult to be sure of

the timing of inclusion formation relative to the mineral precipitation events of interest (Wilkinson, 2001). Furthermore, in most instances, an independent fluid pressure constraint is required to correct measured T_h values to true trapping temperatures.

Although generally applied to low-temperature environments (<50°C; Affek, 2012), the "clumped isotope" carbonate geothermometer ($T\Delta_{47}$) allows the temperature of precipitation to be obtained from any carbonate phase (Eiler, 2007) to temperatures exceeding 250°C (Kluge et al., 2015; Bonifacie et al., 2017). $T\Delta_{47}$ calculations rely on measurements of the degree of ordering of rare 13C and 18O isotopes in the carbon-

[†]Corresponding author: e-mail, steven.hollis@ed.ac.uk

ate mineral lattice (Eiler, 2007). The degree of "clumping" (or relative number of $^{13}C^{18}O$ bonds) is an inverse function of temperature, with an increasingly random (stochastic) distribution at higher temperatures (Eiler, 2007). With falling temperature, clumping of heavy isotopes is progressively favored, as the vibrational energy of the bond is lower than that of the corresponding light-light bond (^{12}C-^{16}O; Wang et al., 2004; John, 2018). In addition to providing $T\Delta_{47}$ for carbonate precipitation, carbonate $\delta^{13}C$ and $\delta^{18}O$ are simultaneously determined. This allows fluid $\delta^{18}O$ in equilibrium with the carbonate to be directly calculated rather than modeled.

Several recent studies have shown that the clumped method can reproduce geologically accurate temperatures and fluid $\delta^{18}O$ values from dolomitized carbonate basins (Honlet et al., 2018; Came et al., 2017; MacDonald et al., 2018; Mangenot et al., 2018a; Chang et al., 2020; Hu et al., 2022), though few studies have applied the technique to ore-forming systems (Mering et al., 2018; Dennis et al., 2019; Quesnel et al., 2022). As carbonate minerals crystallize throughout the development of many hydrothermal systems, clumped isotope analysis presents a new tool for the determination of fluid temperatures and $\delta^{18}O$.

The Irish Midlands is a world-class Zn-Pb ore field, hosting one of the highest concentrations of zinc per square kilometer on Earth (Singer, 1995). In the Rathdowney trend of the southern Irish ore field, Zn-Pb mineralization is hosted in Lower Carboniferous (Courceyan to lower Chadian) ramp and near-shore limestones of the Waulsortian Limestone Formation, as typified by the Lisheen deposit (Fig. 1; Shearley et al., 1995; Hitzman et al., 2002; Fusciardi et al., 2003; Wilkinson et al., 2005b). The giant Navan deposit and a number of smaller prospects occur in the shallow marine facies of the Navan Group farther north (Anderson et al., 1998; Blakeman et al., 2002; Ashton et al., 2015; Yesares et al., 2019). It is well established that these orebodies formed due to mixing of warm, metal-bearing fluids equilibrated with Lower Palaeozoic basement (Everett et al., 1999a, 2003; Wilkinson et al., 2005a; Walshaw et al., 2006) with sinking, cooler, hypersaline brines (Wilkinson and Hitzman, 2015). Five major deposits have been mined and over 20 prospects discovered (Fig. 1), with deposits showing varying degrees of hybrid characteristics in a spectrum between carbonate-hosted sedimentary exhalative (SEDEX) and Mississippi Valley-type (MVT) styles (Andrew, 1986; Hitzman, 1986; Wilkinson, 2014).

To further understand processes associated with fluid mixing and mineralization in the Irish ore field, many studies have investigated fluid inclusions (reviewed in Wilkinson, 2010) and isotope systematics (C, O, H, Rb-Sr, Sm-Nd) of carbonate phases (e.g., Samson and Russell, 1987; Hitzman et al., 1992, 1998; Everett, 1999; Wilkinson et al., 2005a; Walshaw et al., 2006; Menuge et al., 2007; Ashton et al., 2015; Yesares et al., 2019). The Irish ore field is therefore an ideal place to not only test the applicability of clumped isotope analysis on a hydrothermal system, but also fill gaps in our knowledge where fluid inclusions are not available. This is particularly true for several critical pre-ore and ore-stage carbonate phases that rarely contain fluid inclusions large enough for accurate T_h measurement (Hitzman et al., 1992, 1998; Braithwaite and Rizzi, 1997; Eyre, 1998; Wilkinson and Earls, 2000; Ashton et al., 2015).

Geology of the Irish Midlands Ore Field

The geology of the Irish ore field has been well described (e.g., Andrew, 1986; Wilkinson, 2003; Ashton et al., 2015; Wilkinson and Hitzman, 2015; Turner et al., 2019). In this paper, we focus on carbonate phases from three parts of the ore field, namely the Rathdowney trend, related hydrothermal veins hosted in Silurian basement near Silvermines, both in the south midlands, and the Navan deposit of the northeast midlands (Fig. 1).

The Rathdowney trend

The Rathdowney trend includes two mined Zn-Pb deposits, Lisheen and Galmoy, and a number of other prospects (e.g., Rapla, Kildare, Gortdrum). The Lisheen deposit is composed of several separate stratabound orebodies (Fig. 1b), which formed in the hanging wall of a network of normal faults (Shearley et al., 1995; Kyne et al., 2019). The deposit was mined from 1999 until December 2015, producing 22.4 million tonnes (Mt) of ore grading 11.63% Zn and 1.96% Pb (Torremans et al., 2018). Mineralization is dominated by pyrite, sphalerite, and galena, with lesser amounts of niccolite, tennantite, marcasite, and chalcopyrite associated with feeder faults (Eyre, 1998; Fusciardi et al., 2003; Wilkinson et al., 2005b; Torremans et al., 2018). Several generations of carbonate have been recognized at Lisheen (Eyre, 1998; Hitzman et al., 2002; Wilkinson et al., 2005b; Yesares et al., 2019; Doran et al., 2022).

The primary host to Zn-Pb mineralization, the Waulsortian Limestone Formation, is composed of several coalesced carbonate mudbanks, deposited during the Courceyan in marine environments at approximately 120 to >300 m below sea level (Hitzman et al., 2002; Wilkinson, 2003). Early, regional dolomitization of the Waulsortian stratigraphy comprises a fine- to medium-grained (<100- to 500-µm), subhedral/euhedral planar (s- or e-type), gray diagenetic dolomite (dol_{1a}) that preferentially replaced micritic components of the host limestone (Gregg et al., 2001; Wilkinson, 2003). This was partially recrystallized to and/or postdated by a coarser (medium to very coarse), white, predominantly nonplanar regional dolomite (dol_{1b}) that also infilled vuggy porosity (Gregg et al., 2001; Wilkinson, 2003). At Lisheen, the entire Waulsortian Limestone Formation is dolomitized, in addition to nonargillaceous beds in the overlying Crosspatrick Formation (Shearley et al., 1995; Eyre, 1998). Regional dolomite is well developed on both sides of the main Killoran and Derryville faults that bound the Lisheen orebodies to the south (Shearley et al., 1995; Fig. 1b).

Following the regional dolomitization event(s), substantial hydrothermal alteration resulted in several dolomite phases that have crosscut, cemented, brecciated, and replaced the regional dolomite (Fig. 2). Surrounding the massive sulfide orebodies, clasts of regional dolomite (with irregular and diffuse margins) can be found within a matrix of finely crystalline, planar-euhedral black dolomite (dol_2 of Wilkinson et al., 2005b). These black matrix breccias (BMBs) are believed to have formed in situ by hydrothermal replacement and dissolution-collapse, and typically envelop orebodies (Wilkinson and Earls, 2000; Hitzman et al., 2002; Wilkinson et al., 2005b, 2011; Figs. 1d, 2a). In the hanging walls of orebodies, planar to nonplanar white dolomite (dol_3) forms the cement
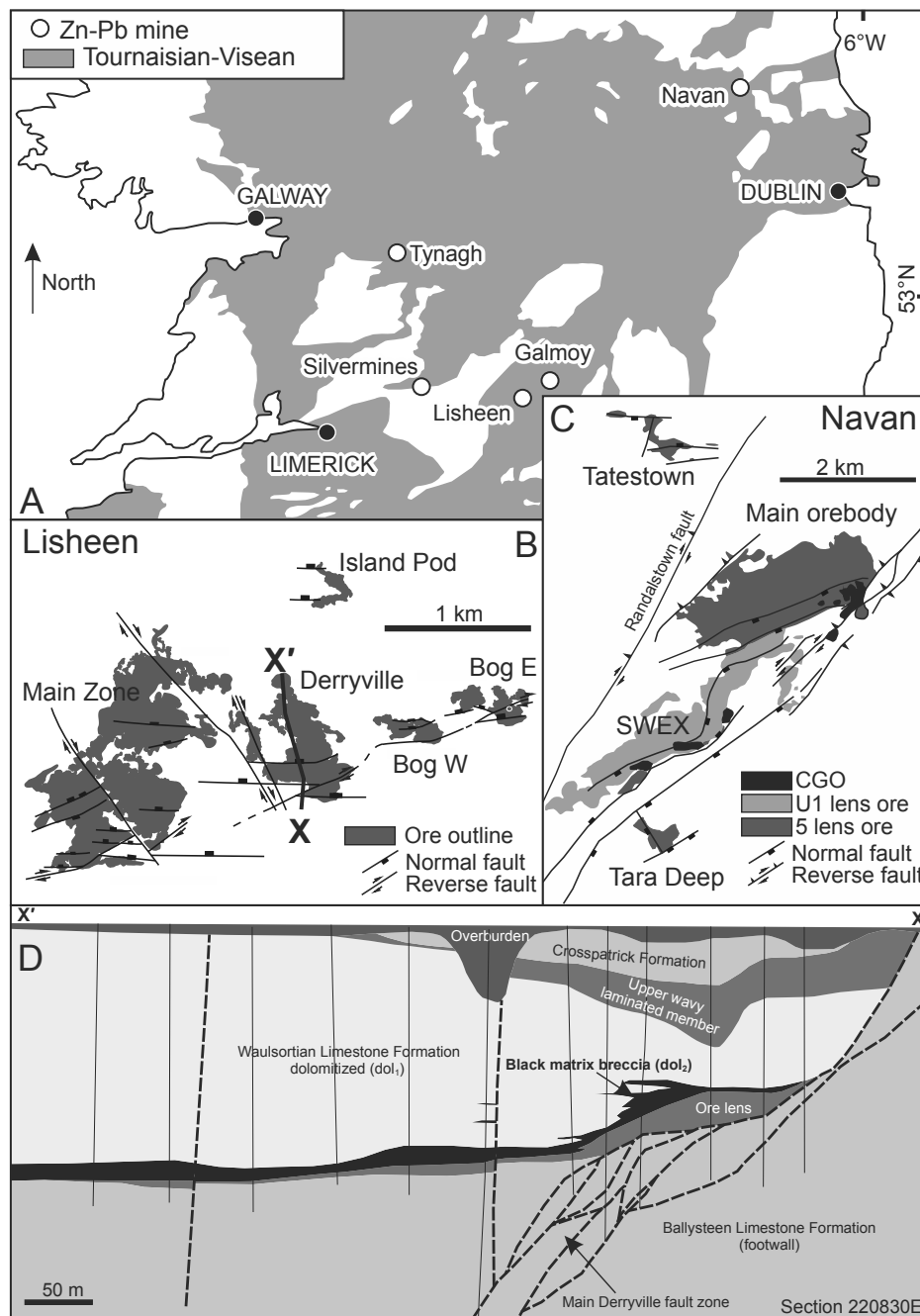
Fig. 1. (A) Distribution of Tournaisian-Visean limestones in central Ireland with the location of mined carbonate-hosted Zn-Pb deposits (after Wilkinson et al., 2011). Birdhill Quarry is located ~15 km west-southwest of Silvermines. (B-C) Projection to surface of the Lisheen and Navan orebodies with major faults indicated (after Kyne et al., 2019; Yesares et al., 2019). (D) Cross section (line of section shown on Fig. 2b) through the Derryville orebody, Lisheen deposit (after Wilkinson et al., 2005b, 2011), showing black matrix breccia (BMB; Fig. 2a) development, which envelops mineralization at the base of regionally dolomitized (dol_1) Waulsortian limestones. White matrix breccias (WMBs; Fig. 2b) form in the hanging wall to mineralization. Additional petrographic images are provided as Appendix Figure A1. Abbreviations: CGO = conglomerate group ore, SWEX = South West Extension.

of white matrix breccias (WMBs; Eyre, 1998; Hitzman et al., 2002; Wilkinson, 2003; Wilkinson et al., 2011; Fig. 2b). These breccias extend over an area approximately four times that of the underlying ore (Hitzman et al., 2002). Clasts of $dol_{1(a+b)}$ in the WMBs are angular to subrounded, and contacts between WMBs and BMBs are usually sharp (on the

order of a few cm: Wilkinson et al., 2011). Post-main ore-stage carbonates include ferroan dolomite (dol_4), veins of pink dolomite (dol_5), and multiple generations of late calcite (cal_6, cal_7) (Figs. 2c-d). Doran et al. (2022) described ore-stage carbonates intergrown with sphalerite in the Island Pod orebody (Fig. 1b).
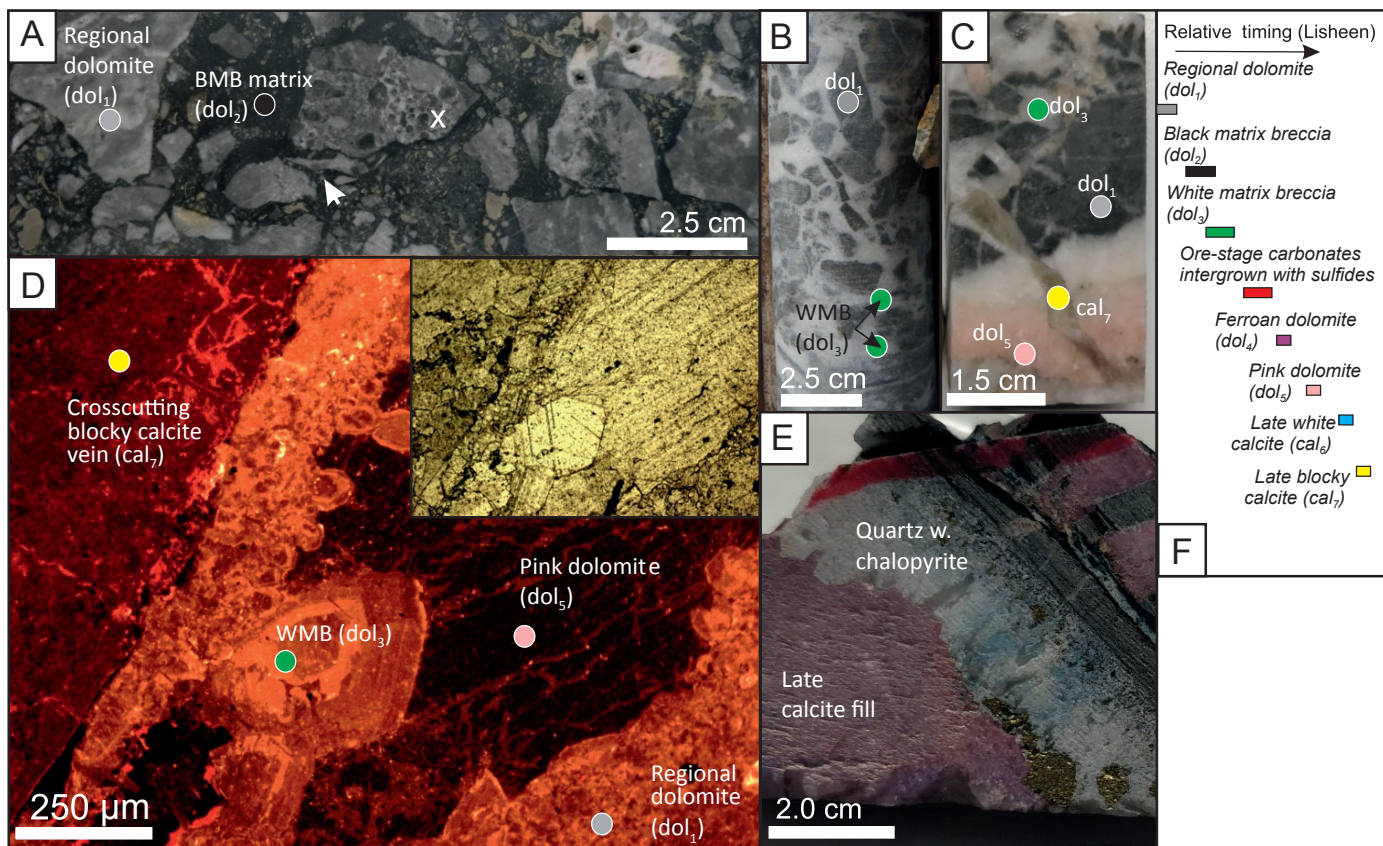
Fig. 2. Representative images of carbonate phases analyzed. (A) Hydrothermal black matrix breccia insert (BMB), Lisheen, with corroded clasts (arrow) of regional dolomite. Some clasts show evidence for multiple brecciation events (clast labeled x). (B) White matrix breccia (WMB) from the hanging wall of the Island Pod orebody, Lisheen. (C) Sample SPL053 containing several carbonate generations from Island Pod. (D) Cathodoluminescence image of sample SPL053 (transmitted light image is inset). (E) Stained quartz-carbonate basement veins, Navan, containing chalcopyrite in early quartz. Dolomite and calcite paragenesis for the Lisheen deposit is according to Wilkinson et al. (2005b), Yesares et al. (2019), and Doran et al. (2022).

The Galmoy deposit lies ~10 km east-northeast along host-rock strike from Lisheen. It contained reserves of 6.9 Mt ore grading 11.5% Zn and 1.3% Pb and was mined from 1997 to 2012. Like Lisheen, it is hosted in Waulsortian limestones, specifically where they have been dolomitized both regionally and later during formation of the rock matrix breccia, a unit very similar to the Lisheen black matrix breccia (Doyle et al., 1992; Doyle and Bowden, 1995). As at Lisheen, a white matrix breccia sealed by dolomite typically overlies the ore-hosting rock matrix breccia. Galmoy consists primarily of Zn-Pb ore-bodies and is bounded to the south by the same major normal fault system as Lisheen.

Veins in pre-Carboniferous basement

Throughout the Irish Midlands, the Lower Carboniferous carbonate sequence hosting the base metal mineralization conformably overlies a clastic, mainly red sandstone, sequence of Devonian to earliest Carboniferous age that thickens from <40 m in the northeast to as much as 200 m in the southwest midlands (Philcox, 1984). Where its base is exposed, mostly in the southwest midlands, this clastic sequence lies unconformably on Silurian low-grade metasediments that host quartz-carbonate-sulfide hydrothermal veins. Structural analysis reveals their formation under a NE-SW–oriented dextral

transtensional regime, consistent with a Lower Carboniferous age (Everett et al., 1999a). These have been interpreted as fluid, and especially dissolved metal, feeder structures to Lower Carboniferous Zn-Pb mineralization, through fluid inclusion and Sr-H-C-O isotope data (Everett et al., 1999a; Wilkinson et al., 2005a). In this study, carbonate from a vein from Birdhill Quarry (~15 km west-southwest of Silvermines) has been studied, along with veins in Silurian basement to the Navan orebody from outcrop and drill core (Fig. 1). Basement veins from Birdhill are described in detail by Everett et al. (1999a), with that analyzed here consisting of type 2 (quartz-calcite ± sphalerite, galena, chalcopyrite, pyrite, barite). The sampled basement veins at Navan are typically 0.5 to 10 cm thick. They are composed of early coarse euhedral quartz-chalcopyrite margins and later calcite and dolomite fills and were sampled from outcrop at Beaupark (northeast of Navan) and in drill core.

The Navan ore deposit

The largest carbonate-hosted base metal orebody in Ireland was discovered and developed at Navan in the 1970s, with production commencing in 1977. Including the satellite Tara Deep orebody, premining reserves stand at 145 Mt grading 7.5% Zn and 1.7% Pb (Andrew, 2023). The Navan deposit and

a number of smaller prospects occur as stratabound, shallow marine oolitic and bioclastic limestones of the Navan Group Pale Beds (Anderson et al., 1998; Blakeman et al., 2002; Ashton et al., 2015; Yesares et al., 2019). These formations lie stratigraphically below the Waulsortian limestones that host the Rathdowney trend deposits, but all form part of a continuous stratigraphic sequence of Courceyan age.

In this paper, we do not present data from the main Navan orebody or overlying subeconomic mineralization but from carbonate veins from the hanging wall of the Randalstown fault (northwest of the South West Extension orebody; Fig. 1c). The Randalstown fault is a northeast-southwest dextral reverse fault with a reverse throw of about 200 m and a dextral displacement of at least 800 m (Ashton et al., 2015). The timing of fault movement is uncertain, possibly late Carboniferous/Variscan, but it is seen to postdate formation of the main Navan orebody. The calcite and dolomite veins, contemporaneous with fault movement, contain coarse honeyblende sphalerite interpreted as remobilized from the main orebody based on its S isotope composition (Marks, 2015). The veins are typically 0.5 to 10 cm thick and crosscut earlier veins that have brecciated the host rock. Occasional fine-grained galena and/or pyrite is present along the margins of the sphalerite (Marks, 2015).

Methods

Sample selection

To provide supporting evidence that the clumped isotope geothermometer (TΔ_{47}) records accurate and geologically meaningful temperature estimates, several existing samples containing well-characterized, two-phase fluid inclusion populations from the Irish ore field (Eyre, 1998; Lee, 2002; Marks, 2015; Wilkinson, 2003, 2010) were subjected to clumped C-O isotope analysis, in addition to new samples collected from drill core at Lisheen and Navan (Fig. 2). Samples from Lisheen included the two generations of regional dolomite (dol$_{1a}$, dol$_{1b}$), black hydrothermal dolomite (dol$_2$) from BMBs, white dolomite (dol$_3$) from WMBs, and a number of post-ore carbonate phases (dol$_5$, cal$_{6,7}$) (Fig. 2). Carbonates intergrown with main ore-stage sulfides (Doran et al., 2022) were too fine grained to sample. Samples analyzed from Navan were restricted to (1) late calcite infilling chalcopyrite-bearing quartz veins cutting Lower Palaeozoic basement rocks (Fig. 2e; sampled from both drill core and outcrop); and (2) calcite veins from the hanging wall of the Randalstown fault (northwest of the South West Extension orebody; Fig. 1c) that contain remobilized honeyblende sphalerite (described in detail by Marks, 2015).

Petrography

Carbonate phases were characterized by optical microscopy and scanning electron microscopy at University College Dublin and imaged using a CITL mk5 cold cathodoluminescence stage mounted on a Nikon 50i microscope at Imperial College London. Additional petrographic images are provided as Appendix Figure A1. Fluid inclusion T_h measurements were acquired on inferred primary two-phase (liquid-vapor) fluid inclusions on doubly-polished wafers at University College Cork. Measurements were made using a Linkam temperature-controlled microscope stage combined with an Olympus BX50 microscope and a 16-megapixel digital camera. Precision on individual measurements was better than ±0.5°C.

Clumped isotope analysis

Clumped C-O isotope analysis of the carbonates was undertaken primarily at the University of East Anglia (UEA), with several samples also analyzed at the University of Colorado Boulder (UCB) in the CU Boulder Earth Systems Stable Isotope Lab (CUBES-SIL; RRID: SCR_019300). For the initial UEA data set (August 2016), carbon dioxide was produced by reacting 3 to 5 mg of carbonate powder with 102% orthophosphoric acid in vacuo at 25°C for a period of 12 hours for calcite and 5 days for dolomite. Subsequent samples (February 2018) were reacted at a temperature of 87°C for 20 minutes. The evolved CO_2 was collected by cryodistillation according to the methodology outlined by Dennis et al. (2019). Potential hydrocarbon and chlorocarbon contaminations were stripped using a static porapak Q packed column with cryogenic transfer at –20°C for 90 minutes. The trap was baked out between samples at 130°C for 30 minutes. Sample gases were analyzed for their isotope ratios on a custom-built MIRA (multiple isotope ratio analyser) dual-inlet mass spectrometer described in Kirk (2017) and Dennis et al. (2019).

Analyte gases were measured on the UEA MIRA mass spectrometer using the analysis and data handling protocol described in detail in Dennis et al. (2019). Each measurement consisted of four acquisitions of 20 sample-reference pairs with a 20-second integration period for each sample or reference cycle and a 10-second dead time after switching of the changeover valve. Between each acquisition, the sample and reference gases were balanced to a major beam intensity of 7.5 × 10^{-8} A. Typical internal measurement precisions were <0.001‰ for δ^{45} and δ^{46}, <0.008‰ for δ^{47}, and <0.03‰ for δ^{48}.

Data quality and long-term measurement uncertainty at UEA were monitored by daily measurement of the UEAC-MST Carrara marble standard over the period of study. External precision (Δ_{47}) for sample analysis was ±0.014‰, which corresponds to temperature uncertainties of ±4.8°C at 25°C, rising to ±19°C at 200°C (Dennis et al., 2019). Sample contamination is expressed through high Δ_{48} and Δ_{49} (Eiler and Schauble, 2004). As the presence of trace sulfides in samples can lead to high Δ_{48} due to the presence of $^{32}S^{16}O$, we applied a strict Δ_{48} cutoff value of +0.15‰. Mass 49 was also monitored for evidence of contamination (after Dennis et al., 2019). It is important to note that the UEA MIRA mass spectrometer is linear for Δ_{48} measurements, and the Δ_{48} value reported is that determined using the mass spectrometer working reference gas, which was equilibrated with water at 20°C. Thus, carbonates are expected to have small negative values. In practice, most samples had measured Δ_{48} values close to zero and usually slightly negative, indicating that sample analyte gases were not contaminated (Dennis et al., 2019). The raw mass spectrometer data were handled in accordance with the detailed description provided by Dennis et al. (2019). In order to report Δ_{47} values with respect to the carbon dioxide equilibrium scale (CDES) reference frame, a transfer function was constructed using 1,000°C heated and 20°C water-equilibrated gases.

A subset of the same samples was also analyzed in the CUBES-SIL using a Thermo Scientific 253+ dual inlet mass

spectrometer. Carbonate powders were reacted in 105% orthophosphoric acid in a common acid bath at 90°C while being pumped through a –75°C water trap to a liquid nitrogen cold trap for 25 minutes. The samples were then further cleaned by passage through silver wool and a –20°C Poropak Q GC (4' length; 1/8" diameter) at ~13 ml/m helium flow. The frozen gas was cleaned of any condensable phases by pumping and then unfreezing and refreezing. The samples were then warmed to ~25°C and expanded directly into the bellows.

Each Δ_{47} value from UCB consisted of a single analysis that is composed of nine measurement acquisitions, each containing seven sample/reference cycles. Samples are typically run in triplicate to achieve sufficient precision, but the number of contaminated samples created analytical challenges, so single analysis of samples was carried out with the primary intent of comparison with the UEA data. Typical internal measurement precisions for clean samples were <0.007‰ for δ^{45} and δ^{46}, <0.02‰ for δ^{47}, and <0.06‰ for δ^{48}. Heated (1,000°C) and equilibrated (25°C) gases were measured, and the heated gases were used to correct Δ_{47} values for nonlinearity. Δ_{47} values were converted to the CDES reference in two ways: using the 1,000°C and 25°C gases (primary approach of Dennis et al., 2011) and using carbonates standards (secondary approach; Dennis et al., 2011). After comparison, the two approaches yielded slightly different equilibrium transfer functions. The carbonate standards method (see App. 1) yielded smaller residuals for the expected values of the standards, so these values are reported here. This approach and all plots are provided as appendices. Sample cleanliness at UCB was determined using Δ_{48} values; Δ_{48} values were first corrected for nonlinearity using the heated gas Δ_{48} values. By definition, all carbonate data should fall between the 1,000° and 25° gas lines, so data were considered dirty and therefore excluded if they fell higher than the predictive interval of the equilibrated gas Δ_{48} line. Samples that fell above the Δ_{48} equilibrated gas line but below the predictive uncertainty window were noted as possibly contaminated and compared to other clean data (see Appendixl).

$\delta^{18}O$ values were corrected using the carbonate-phosphoric acid fractionation factors of 1.01182 (dolomite at 25°C; Rosenbaum and Sheppard, 1986), 1.01025 (calcite at 25°C; Friedman and O'Neil, 1977), 1.00931 (dolomite at 90°C; Rosenbaum and Sheppard, 1986), and 1.0084 (calcite at 90°C; Swart et al., 1991). All $\delta^{18}O$ values are reported relative to international standard Vienna-standard mean ocean water (V-SMOW). The bulk $\delta^{18}O$ isotope signature of any given carbonate phase is dependent on fluid $\delta^{18}O$ and the fractionation factor between the crystallizing phase and water. Fluid $\delta^{18}O_{V-SMOW}$ values for clumped data were calculated according to Kim and O'Neil (1997) for calcite and Horita (2014) for dolomite.

The clumped isotope palaeothermometer (Δ_{47}) is mathematically defined according to equation 1:

$$\Delta_{47} = (R^{47}_{measured}/R^{47}_{stochastic} - 1)\,1000 \qquad (1)$$

A dozen or so published equations exist to calibrate Δ_{47} against temperature (Ghosh et al., 2006; Kluge et al., 2015; Bonifacie et al., 2017; Dennis et al., 2019; Petersen et al., 2019). Differences between calibrations are laboratory de-

pendent. For the UEA data set, we used the in-house temperature calibration as described in Dennis et al. (2019). This calibration was determined using natural biogenic carbonates (bivalves and foraminifera) and travertine samples collected from sites with well-characterized formation temperatures and reacted at 25°C (Kirk, 2017; equation 1). For samples reacted at 87°C, the temperature calibration is corrected by the offset 0.062 in the clumped isotope fractionation factor that was empirically determined in the UEA lab (equation 2). The offset is indistinguishable from that theoretically determined by Guo et al. (2009). For UCB analyses, as no in-house temperature equation is available, temperature data are reported according to recently published universal calibrations of Bonifacie et al. (2017) and Petersen et al. (2019) in addition to Dennis et al. (2019; equation 3). The latter two equations produce almost identical temperature estimates for the data from UCB and are justified given that we use ETH standards to correct the data and so the CDES values are close to those for the Intercarb-carbon dioxide equilibrium scale (ICDES) reference frame (Bernasconi et al., 2021). Furthermore, the Δ_{47}-T calibration provided in Anderson et al. (2021) and reported relative to the ICDES reference frame is extremely similar to Petersen et al. (2019) and indistinguishable within measurement uncertainty from the UEA calibration (App. Table A1):

$$\Delta_{47} = \left(\frac{0.0389 \cdot 10^6}{T^2}\right) + 0.2139; \qquad (2)$$

$$\Delta_{47} = \left(\frac{0.0389 \cdot 10^6}{T^2}\right) + 0.1519 \qquad (3)$$

Results

Carbonate phases of the Rathdowney trend

TΔ_{47} values between ~130° and 180°C were obtained for phases of regional dolomite at UEA that predate sulfide mineralization across the Irish ore field (Fig. 3). High TΔ_{47} for early, fine, gray replacive dolomite (dol$_{1a}$) were obtained from Lisheen (mean 163° ± 15°C, n = 2), and a sample of dolomitized Waulsortian Limestone collected ~7 km southeast of Lisheen (mean TΔ_{47} 177° ± 16°C; n = 2) that has low whole-rock base metal contents (61 ppm Zn; 3 ppm Pb; Wilkinson et al., 2011) and is distal to all known mineral deposits. The latter sample, repeated by a single analysis at UCB, yielded higher temperatures of 212° to 258°C according to $\Delta_{47} - T$ calibrations of Bonifacie et al. (2017), Dennis et al. (2019), and Petersen et al. (2019), respectively (discussed below). A relatively high TΔ_{47} of 137° ± 12°C was also obtained for a sample of coarse white regional dolomite (dol$_{1b}$) from the sample regional outcrop ~7 km southeast of Lisheen. Samples of regional dolomite dol$_{1(a + b)}$ yielded high calculated fluid $\delta^{18}O$ values (4.6 to 12.8‰).

Clumped isotope analysis of dol$_2$ from BMB dolomite matrix at both UEA and UCB resulted in very high levels of contamination (Δ_{48} >6‰) likely due to the presence of abundant fine-grained sulfides. Therefore, all BMB data were discarded because TΔ_{47} values are considered unreliable (Petersen et al., 2016; Bergmann et al., 2018). Analysis of BMB material also resulted in high Δ_{48} of several clean (i.e., nonsulfide–bearing) carbonates analyzed subsequently at both laboratories. These results were similarly discarded.
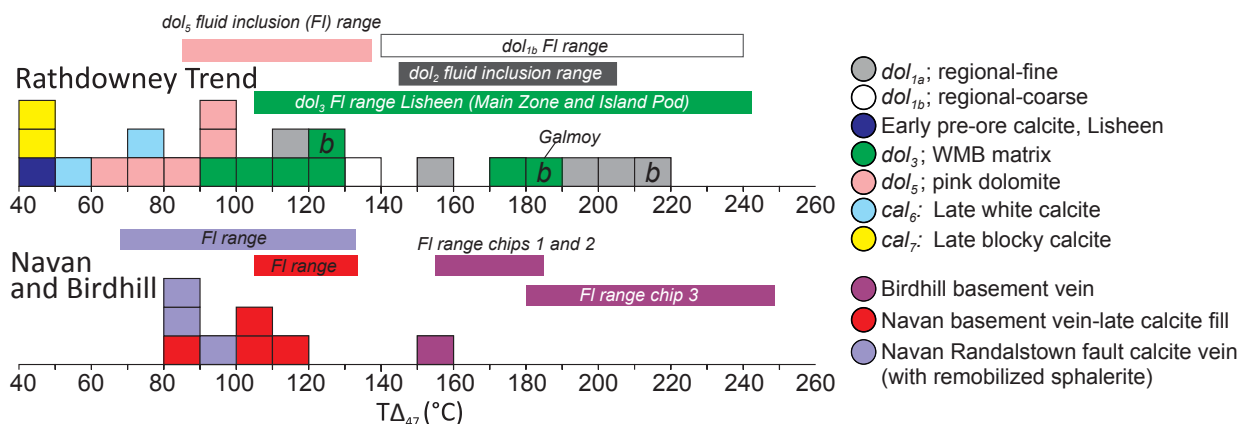
Fig. 3. Histograms of TΔ_{47} for carbonate phases measured from the Rathdowney trend (including the Lisheen and Galmoy deposits), and basement vein samples from Navan and Birdhill. Fluid inclusion ranges are shown for comparison, including data from Eyre (1998), Everett (1999), Lee (2002), Wilkinson (2010), and Marks (2015). Each box represents one analysis. For UCB data, the Bonifacie et al. (2017) temperatures are shown (b in box). Abbreviations: FI = fluid inclusion, WMB = white matrix breccia.

Coarse-grained white dolomite (dol$_3$) from WMBs above the Island Pod orebody at Lisheen yielded a TΔ_{47} range of 98° ± 9° to 172° ± 16°C (Fig. 3). A replicate of one sample (SPL053D) yielded a temperature of 98° ± 9°C at UEA and temperatures between 121° and 136°C from UCB according to different temperature calibrations (see App. Table A1). Fluid inclusions from Island Pod WMBs were too small for accurate analysis, apart from sample SPL056B, which yielded a TΔ_{47} value of 118°C and mean T$_h$ value of 116°C (range 106°–134°C). A high temperature was obtained from clumped isotope analysis for a sample of dol$_3$ from WMB from Galmoy (UCB: 188° to 225°C using T-Δ_{47} calibrations of Bonifacie et al., 2017, Dennis et al., 2019, and Petersen et al., 2019; Fig. 3); this phase has previously yielded a mean T$_h$ of 174°C (range 129°–222°C; Lee, 2002). No systematic variation was apparent in WMB Δ_{47} temperatures with proximity to mineralization, based on the limited vertical sampling of ~80 m of drill core above massive sulfides (n = 4). Calculated fluid $\delta^{18}O$ values for samples of WMB range from +0.7 to +10.0‰.

Significantly lower TΔ_{47} values were obtained from post-ore pink dolomite (dol$_5$; 80°–86° ± 8°C), late white calcite (cal$_6$; 63° ± 7°C), and crosscutting late blocky calcite (cal$_7$; 42°–43° ± 6°C) (Fig. 3). These samples yielded significantly lower fluid $\delta^{18}O$ values than all other samples analyzed from Lisheen (pink dolomite –0.7 to +3.8‰; late white calcite –3.9 to –1.3‰; late blocky calcite –6.2 to –3.5‰). Newly measured fluid inclusion T$_h$ values for three samples of pink dolomite from Lisheen (App. Table A1) were ~100°C, with one additional sample yielding a higher mean T$_h$ of ~123°C. These T$_h$ values are similar to those previously reported from elsewhere across the Irish ore field (91° to 137°C; Gregg et al., 2001; Wilkinson, 2010; Fig. 3). No fluid inclusions suitable for analysis were observed in late calcites from Lisheen.

Constraints from the Navan deposit and regional basement veins

Two suites of samples were analyzed from Navan (Fig. 3). The first was late calcite fill associated with chalcopyrite-bearing quartz veins (TΔ_{47} of 86° ± 8° to 91° ± 9°C; mean T$_h$ of 116° to 134°C) cutting Lower Paleozoic basement rocks. These

yielded fluid $\delta^{18}O$ values of –0.8 to +1.2‰. The second suite of samples analyzed from Navan came from calcite veins from the hanging wall of the Randalstown fault (northwest of the South West Extension orebody; Fig. 1c) containing remobilized sphalerite (Marks, 2015). These yielded TΔ_{47} values of 77° ± 8° to 110° ± 10°C; new, near-identical mean T$_h$ values of 81° to 109°C; and fluid $\delta^{18}O$ values of –0.9 to +6.0‰. One relatively high temperature analysis was also obtained from a Lower Paleozoic basement-hosted calcite vein from Birdhill (TΔ_{47} = 155° ± 14°C; fluid $\delta^{18}O$ +6.9‰), which has yielded T$_h$ values of 140° to 249°C (mean 194°C; n = 32; Everett, 1999).

Discussion

Correlations between fluid inclusion and clumped isotope thermometry

In the Irish ore field, T$_h$ values are unlikely to be significantly different to trapping temperatures (detailed in Wilkinson and Earls, 2000; Wilkinson, 2010). Although estimation of trapping temperature from T$_h$ is a function of fluid pressure at the time of fluid trapping, the different models for burial depth in Irish-type systems (Andrew and Poustie, 1986; Hitzman and Beaty, 1996) yield a fairly narrow range of temperature corrections of between +1.1°C and +12.2°C, with recent literature favoring the former (Wilkinson and Hitzman, 2015). The assumption that T$_h$ values are not significantly different to trapping temperatures is supported by stable isotope geothermometry on mineralized Lower Palaeozoic-hosted veins (Everett et al., 1999b).

A comparison of mean fluid inclusion T$_h$ (henceforth considered a good proxy for trapping temperature in this study) from the same samples analyzed for clumped C-O isotope compositions shows a close match between TΔ_{47} and T$_h$. This is consistent with several other recent studies comparing hydrothermal TΔ_{47} and T$_h$ measurements worldwide (Honlet et al., 2018; Came et al., 2017; Mangenot et al., 2018a; Mering et al., 2018; Doran, 2021). In the Irish ore field, matches between TΔ_{47} and T$_h$ are particularly strong for dolomites from Lisheen, and calcites from the hanging wall of the Randalstown fault at Navan, as demonstrated in Figure 4. For ex-

ample, paired $T\Delta_{47} - T_h$ values for individual samples from the hanging wall of the Randalstown fault are 99° to 91°C (sample A2), 77° to 81°C (sample 15), and 110° to 109°C (sample 16). Sample SPL056B of dol_3 from a WMB above the Island Pod orebody yielded a $T\Delta_{47}$ of 118° ± 11°C and mean T_h value of 116°C (range 106° to 134°C).

$T\Delta_{47}$ values obtained here are also comparable to T_h values reported from similar carbonate phases elsewhere across the Irish ore field. For example, $T\Delta_{47}$ values for dol_3 from WMBs above the Island Pod orebody (90°–160°C) are comparable with T_h constraints from WMBs above the Main Zone orebody at Lisheen (Main Zone orebody: 112°–241°C), Galmoy (99°–225°C; Lee, 2002), and other parts of the Rathdowney trend (see Eyre, 1998; Wilkinson, 2010). A high $T\Delta_{47}$ value for dol_{1b} of 137° ± 12°C from UEA is similar to but at the low end of the range of T_h values reported by a number of previous workers (~140°–240°C: Eyre, 1998; Wilkinson and Earls, 2000; Gregg et al., 2001; Wilkinson, 2003; Wilkinson et al., 2011).

Although many of our data are within error of the 1:1 line, some $T\Delta_{47}$ values are ~30° to 40°C lower than mean T_h values (Fig. 4). These data are predominantly from the late calcite fill in basement vein samples at Navan (associated with earlier quartz-chalcopyrite), plus the single calcite vein sample from Birdhill (BIR4), one Lisheen pink dolomite sample (SPL049), and one sample of early pre-ore calcite from Lisheen (SPH070). When not associated with high Δ_{48}, mismatches between T_h and $T\Delta_{47}$ can be interpreted to reflect burial recrystallization or solid-stage reordering (e.g. MacDonald et al., 2018; Drummond, 2021), or possibly the inadvertent measurement of nonprimary fluid inclusions. These scenarios will be discussed later.

Although most of our analyses were completed at UEA, a number were also reanalyzed at UCB. It is important to note that the higher temperatures obtained at UCB for the repeat samples of fine-grained regional dolomite (dol_{1a}, sample D1A) and WMB (SPL053D) are outside the error of the UEA analyses (App. Table A1). As these samples are demonstrably clean, this is not an issue of contamination. These interlaboratory temperature differences are less important when at the lower temperature end but become magnified at higher temperatures (~200°C). The slightly higher UCB temperatures may reflect either (1) geologic heterogeneity in the drilled and analyzed material (considered unlikely due to sample homogenization prior to analysis); (2) interlab variations in methodology and/or the choice of T - Δ_{47} calibration used for UCB data; or (3) that they are single analyses and so are prone to analytical variability. From the three temperature calibrations provided, the Bonifacie et al. (2017) equation yields temperatures much closer to those obtained by UEA and measured T_h values (Fig. 3). The Bonifacie et al. (2017) calibration is therefore favored here for the UCB data set.

Early dolomitization events

We record high $T\Delta_{47}$ values for both the fine-grained gray replacive (dol_{1a}) and the coarse white dolomite (dol_{1b}), with the former (Gregg et al., 2001) or both generations (e.g., Hitzman et al., 1998) interpreted to be associated with regional dolomitization of the Waulsortian Limestone in southeast Ireland. No fluid inclusion data have been reported for the fine-grained dol_{1a} (Wilkinson, 2010), although petrographic studies have suggested that this phase is diagenetic, with dolomite crystallization perhaps occurring from an evaporitic brine of seawater origin (Gregg et al., 2001). Thus,
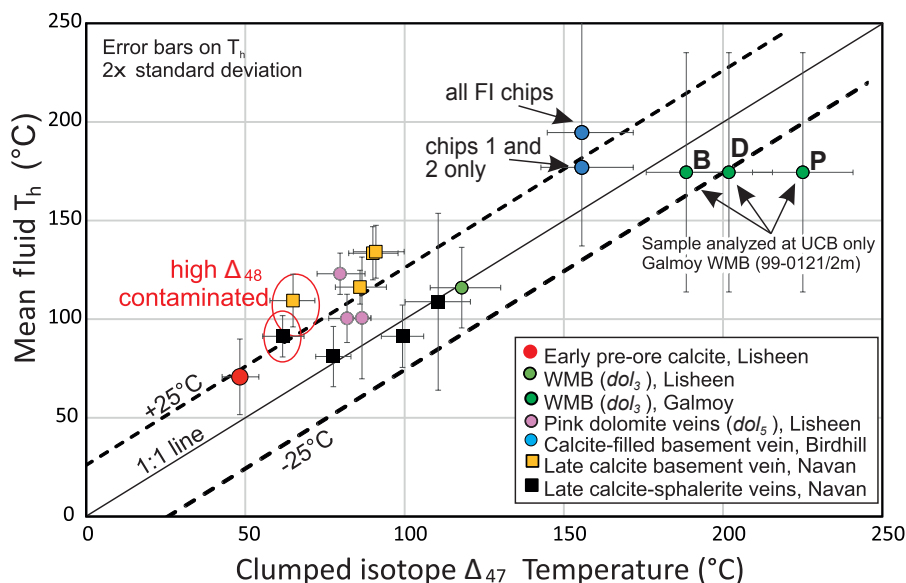

Fig. 4. A comparison of mean fluid inclusion homogenization temperatures (T_h) and $T\Delta_{47}$ for the same samples analyzed by clumped C-O isotopes, including fluid inclusion data of Eyre (1998), Everett (1999), Lee (2002), Wilkinson (2010), and Marks (2015). Dashed lines represent ± 25°C of the 1:1 line. $T\Delta_{47}$ error is calculated from the long-term standard deviation of UEACMST. Contaminated samples with high Δ_{48} will be displaced to the left from true Δ_{47} temperatures. Error bars for fluid inclusion values are two standard deviations of the measured population. Δ_{47} temperatures for sample 99-0121/2m (analyzed only at UCB) are reported according to the $\Delta_{47} - T$ calibrations of Bonifacie et al. (2017; B), Dennis et al. (2019; D), and Petersen et al. (2019; P). For sample BIR4 (Birdhill basement vein), two mean T_h values are provided—using all data from three fluid inclusion chips, and a mean for two chips of lower temperature (see discussion). Abbreviations: FI = fluid inclusion, WMB = white matrix breccia.

the high temperatures obtained from dol_{1a} (UEA and UCB: 118°–212°C) are unlikely to be primary. They are also unlikely to be caused by subsequent burial and closed-system solid-state reordering because late ore-stage carbonates (both calcite and dolomite) were also analyzed from these specimens (e.g., SPL053; Fig. 2c-d) and these retain primary low temperatures (42°–96°C; App. Table A1) that are consistent with fluid inclusion T_h where available.

Gregg et al. (2001) presented a detailed petrographic, fluid inclusion, and O-C account of carbonate generations across the Irish ore field. They proposed that where the early dol_{1a} was exposed to hydrothermal fluids, it underwent neomorphic recrystallization to coarser crystalline, planar, and nonplanar dolomite with lower $\delta^{18}O$ values. This is broadly consistent with our elevated $T\Delta_{47}$ data, which we therefore also interpret in terms of recrystallization due to the hydrothermal activity that resulted in precipitation of the coarse white dolomite phase (dol_{1b}), and in some cases dol_3, in the same samples. Data from undolomitized limestones at Galmoy demonstrate a similar effect to that observed in dol_{1a}, and were also interpreted to have been reset to higher $T\Delta_{47}$ due to local hydrothermal activity (Doran, 2021).

The temperature data we report for dol_{1b} from UEA (Fig. 3) is consistent with fluid inclusion homogenization temperatures from this carbonate phase (~140°–240°C; Eyre, 1998; Wilkinson and Earls, 2000; Gregg et al., 2001; Wilkinson, 2003; Wilkinson et al., 2011), suggesting that this phase represents the first manifestation of regionally developed hydrothermal fluid activity in the Irish ore field, associated with the onset of fault-controlled subsidence (Gregg et al., 2001; Wilkinson, 2003). Previous research has suggested that dol_{1b} was precipitated on a regional scale from a remarkably homogeneous fluid, particularly in terms of salinity (Wilkinson and Earls, 2000; Wilkinson, 2010), which has very similar characteristics to fluids associated with Lower Palaeozoic-hosted, quartz-carbonate veins (Everett, 1999; Everett et al., 1999a). Previously published oxygen isotope data from dol_{1b} were consistent with either a low-temperature marine fluid (~60°C for $\delta^{18}O_{fluid}$ 0‰; e.g., Allan et al., 1992) or a higher-temperature hydrothermal water (130°–220°C for $\delta^{18}O_{fluid}$ ~8–10‰; Wilkinson and Earls, 2000). However, the latter scenario is more consistent with the existing fluid inclusion data (Hitzman et al., 1992; Eyre, 1998; Wilkinson and Earls, 2000; Gregg et al., 2001; Wilkinson, 2003, 2010; Wilkinson et al., 2011).

Using clumped isotopes, $\delta^{18}O_{fluid}$ can be calculated rather than modeled. Considering both the fluid inclusion (T_h) and clumped isotope ($T\Delta_{47}$) constraints, the fluid which formed dol_{1b} (and interpreted to reset dol_{1a}) was evidently hydrothermal (Fig. 5), well above any ambient rock temperature at likely burial depths. Significantly, Wilkinson (2003) noted that the upper end of the T_h array for dol_{1b} matches that of dol_3, which forms the cement of WMBs in the hanging wall to Zn-Pb mineralization, and suggested a continuum between the two stages.

Early dolomitization, similar to that in the Irish Midlands, has also been recognized in other Zn-Pb districts worldwide (e.g., Konari and Rastad, 2018). Reactive transport modeling of dolomitization (Yapparova et al., 2017) predicted several general features that are common in the Irish ore field: (1)

elevated temperatures (modeled up to 100°C) were found to greatly increase the rate of hydrothermal dolomitization and dolomite fronts become sharper; (2) inclined faults induce dolomitization in the hanging wall; and (3) the presence of a low-permeability barrier above faults feeding hydrothermal fluids leads to the formation of stratabound dolomitization as opposed to discordant and more massive dolomitization. In Ireland, it is suggested that increased porosity and permeability due to early regional dolomitization ($dol_{1a + b}$) surrounding relay-ramp fault systems helped establish longer-lived hydrothermal circulation and focussed Zn-Pb mineralization at the same sites over an extended period of time (Wilkinson, 2003).

Fluid mixing, rock buffering, dissolution, and breccia formation

$T\Delta_{47}$ values for the coarse white matrix breccia dolomite (dol_3) that formed in the hanging wall of the Lisheen orebody range from 90° to 160°C. The slightly lower $T\Delta_{47}$ (and T_h) values obtained here from the Island Pod, when compared with T_h values from the Main Zone orebody at Lisheen (112°–241°C; mean 180°C; Eyre, 1998; Wilkinson, 2010), are consistent with the Island Pod's position as a distal orebody, likely lower fluid temperatures (e.g., absence of significant Cu), and simpler paragenesis (Torremans et al., 2018; Doran et al., 2022), similar to the CW orebody at Galmoy (Eyre, 1998; Wilkinson, 2010). Assuming isotopic equilibrium, these $T\Delta_{47}$ temperatures imply crystallization from fluids with $\delta^{18}O$ values between ~0 and ~8‰ (Fig. 5). Previously reported oxygen and carbon isotope data for WMB samples have been interpreted in terms of fluid-rock interaction between the early Waulsortian dolomite and a hydrothermal fluid (Wilkinson, 2003). The $T\Delta_{47}$-$\delta^{18}O_{fluid}$ data obtained here may be explained either through (1) fluid mixing or (2) buffering of the hydrothermal fluids by such early-formed dolomite (Fig. 5). Each scenario is discussed below.

In the former (not favored) model, WMB clumped isotope data might reflect fluid mixing between a rapidly ascending hydrothermal fluid (170°–210°C; $\delta^{18}O_{fluid}$ +10 to +15‰), and a downwelling, cold hypersaline brine ($\delta^{18}O_{fluid}$ 0 to –10 ‰; Fig 5). Such a model is consistent with the general interpretation of the ore-forming process in the ore field (Samson and Russell, 1987; Wilkinson et al., 2005a; Wilkinson and Hitzman, 2015), but not with reported data from the WMB itself, which is dominated by the high-temperature hydrothermal end member (Wilkinson, 2003; 2010). Mixing between a rapidly ascending hydrothermal fluid and cooler meteoric groundwaters has previously been proposed to explain the distribution of clumped isotope temperatures for mineralization in the Peak District MVT province (Dennis et al., 2019). In their study, centimeter-scale zoned patterns of temperature increase are associated with episodic calcite vein growth, interpreted to reflect repeated pulses of fluid injection (Dennis et al., 2019). The range in temperatures was believed to be due to a range of mixing ratios between two fluid end members: a basin-derived fluid (>100°C) and local meteoric water.

In the second (favored) model, ascending hot and mildly acidic, metal-bearing fluids (170°–260°C, $\delta^{18}O_{fluid}$ +10 to +15‰) came into contact with dolomitized Waulsortian limestones in the hanging walls of normal faults, leading to widespread dissolution and subsequent reprecipitation of hy-
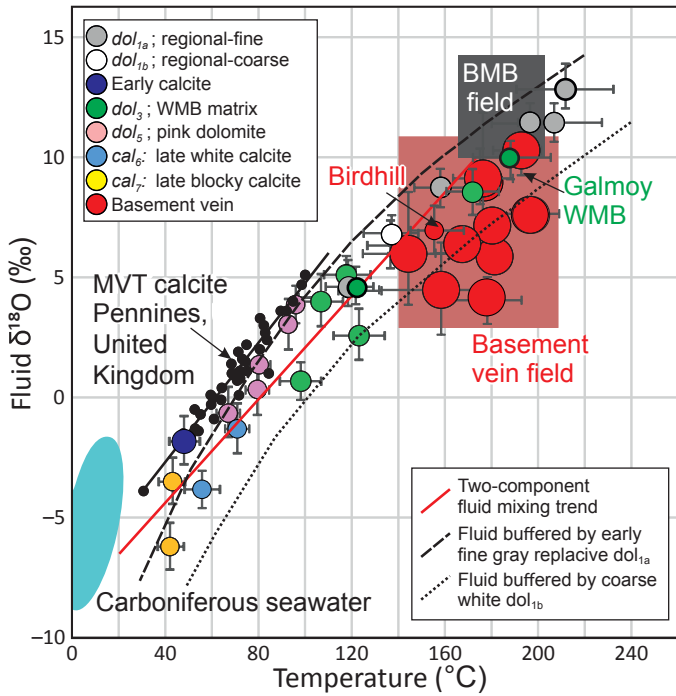
Fig. 5. Fluid δ¹⁸O vs. TΔ₄₇ for all samples analyzed from the southern Irish ore field (including repeat analyses). Analyses from the University of Colorado Boulder (UCB) are reported according to the Δ₄₇–T calibration of Bonifacie et al. (2017), which proves a closer match to University of East Anglia (UEA) replicates (samples SPL53D and D1A) and measured T$_h$ values (e.g., Galmoy white matrix breccia [WMB]; Fig. 3). Large red circles mark basement vein fluid compositions calculated from fluid inclusion T$_h$ and mineral δ¹⁸O data (Everett, 1999). Dashed and dotted curves reflect fluids in isotopic equilibrium with the mean compositions of fine replacive gray regional dolomite (dol₁ₐ; mean δ¹⁸O$_{dol}$ +23.9‰) and coarse white regional dolomite (dol₁ᵦ; mean δ¹⁸O$_{dol}$ +22.3‰), respectively (data from Hitzman et al., 1998). The Irish-type deposit mixing trend is shown by the red solid line (linear regression for samples with fracture filling texture, r² = 0.87). Black matrix breccia (BMB) fluid δ¹⁸O values calculated from fluid inclusion T$_h$ values of Wilkinson and Earls (2000) and δ¹⁸O$_{dol}$ values of Eyre (1998). Clumped isotope data from calcite veins associated with Mississippi Valley-type (MVT) mineralization in the Pennines (small black circles and best-fit solid black line) is shown for comparison (Dennis et al., 2019). The isotopic composition of Lower Carboniferous seawater is calculated for a temperature range of 0° to 20°C using δ¹⁸O$_{mineral}$ values from Veizer et al. (1999; δ¹⁸O$_{calcite}$ = –6 to –1‰ Vienna Pee Dee Belemnite [V-PDB]).

drothermal dolomite. This second scenario is favored based on observed breccia textures across the Rathdowney trend and isotopic compositions. Corroded clasts of regional dolomite occur in BMBs at Lisheen and Galmoy, suggesting the formation of widespread hydrothermal pseudobreccias associated with Zn-Pb mineralization (Fig. 2a; Hitzman et al., 2002; Wilkinson et al., 2005b, 2011). The WMBs most likely formed as collapse breccias associated with significant dissolution of the underlying Waulsortian during mineralization. This is further supported by mass change data and clast rotation in WMBs (Wilkinson et al., 2011). Whereas BMBs have corroded clasts, WMB clasts are generally quite angular and have been cemented by zoned white dolomite crystals (dol₃) with an open-space–filling texture (Figs. 2a, b). Large volumes of the hydrothermal end-member fluid would be required in the lower part of the system to maintain a significantly elevated

thermal anomaly at such shallow levels in the crust (<200 m; Wilkinson et al., 2011). In the hanging wall, where subsidence occurred, cool, downwelling hypersaline brines are interpreted to have mixed with ascending fluids (Wilkinson et al., 2011) to produce relatively wide temperature variations (~70°C) within breccias at the centimeter scale. White matrix breccia dol₃ is suggested to have precipitated from these mixed and cooling "exhaust" fluids. These centimeter-scale temperature variations are apparent in both clumped isotope and fluid inclusion (Wilkinson, 2010) data sets. The curvature of the data array (Fig. 5; also Doran, 2021) is also a better fit to this fluid-rock buffering model than to the fluid mixing model.

The observed and calculated slightly lower fluid δ¹⁸O values, higher temperatures (Everett et al., 1999b; Fig. 5), and strongly negative δ¹³C values (App. Fig. A2) for Lower Palaeozoic basement-hosted veins (e.g., Birdhill) are to be expected for basement-sourced fluids. The Lower Palaeozoic basement is dominated by volcanic and siliciclastic rocks and rising hydrothermal fluids would not have interacted with carbonate rocks.

Samples with discrepancies between TΔ₄₇ and primary T$_h$

Although few researchers have applied clumped C-O isotopes to ore deposits (Dennis et al., 2019; Mering et al., 2018, Doran, 2021), the evidence suggests that robust geothermometry using calcite and dolomite is possible in some mineral systems but not in others (Quesnel et al., 2022). The coherence between TΔ₄₇ and primary T$_h$ of hydrothermal carbonates in our samples suggests that the clumped signature has not been reset by prolonged burial in dolomites from Lisheen or calcite from the hanging wall of the Randalstown fault at Navan. In contrast, late calcite fill from basement veins at Navan and Birdhill and a single sample of early calcite from Lisheen yield systematic offsets between (lower) TΔ₄₇ and (higher) mean T$_h$ by ~30° to 40°C (Fig. 4). Temperature offsets between TΔ₄₇ and T$_h$ have been recorded elsewhere in the literature, in both directions. For example, Honlet et al. (2018) recorded significantly higher TΔ₄₇ temperatures than T$_h$ from the Variscan foreland fold-and-thrust belt in northern Spain, which were attributed to overpressured dolomitizing fluids. This would not occur in the Irish ore field, given the fact that Irish-type deposits formed relatively near the sea floor in water depths of <300 m (Boyce et al., 1983; Wilkinson, 2010; Wilkinson and Hitzman, 2015). In contrast, MacDonald et al. (2018) recorded lower TΔ₄₇ (by 20° to 60°C) than fluid inclusion and well temperatures, interpreted to be due to open-system, burial-related recrystallization. Below we discuss four scenarios that could explain the temperature offsets in these selected samples from the Irish ore field, including burial.

In the first scenario, analytical contamination in the clumped system can result in lower TΔ₄₇ due to higher measured Δ₄₇. However, at UEA we monitored for potential artifacts using the measured Δ₄₈ value. For most measurements this was a negative value, indicating no contamination (e.g., Dennis et al., 2019). Where Δ₄₈ exceeded +0.15‰ we excluded the analysis (see "Methods" section for details). These samples are therefore considered uncontaminated.

Another scenario is that calcite from basement veins at Birdhill and Navan was affected by partial resetting of the clumped bonding due to burial. Given the lack of petro-

graphic evidence for recrystallization in these calcite samples, closed-system, solid-state bond reordering is one possible mechanism for lower $T\Delta_{47}$ than T_h due to burial, rather than open-system isotopic resetting. Drummond (2021) discussed a similar situation in samples from the Tara Deep deposit at Navan, which was explained by reset calcite but only partially reset dolomite. Dickson et al. (2023) also presented evidence for isotopic resetting of the $T\Delta_{47}$ signature of Carboniferous calcite cements from the Isle of Man. Closed-system, solid-state bond reordering in these samples due to burial would be consistent with the lower blocking temperature of calcite than dolomite (Dennis and Schrag, 2010; Lloyd et al., 2018) and that many Lisheen dolomites exhibit a strong $T\Delta_{47}$-T_h match. Apparent equilibrium blocking temperatures in slowly cooled dolomite marbles are notably higher ($\sim$210°–300°C) than in calcite marbles ($\sim$150°–200°C) (Lloyd et al., 2017; Quesnel et al., 2022). However, it is important to note that all samples of calcite from veins in the hanging wall of the Randalstown fault (detailed above) exhibit matches between $T\Delta_{47}$ and T_h within analytical error (Fig. 4). It is unclear why only some calcites would be affected, as the vertical differences in burial depth between the basement veins, Tara Deep (Drummond, 2021), and above the South West Extension orebody would be minimal.

A perhaps more likely explanation for the Navan basement samples with lower $T\Delta_{47}$ than T_h values may lie in the common failure for vapor bubbles to nucleate in low-temperature fluid inclusions (Wilkinson, 2017). This could have been compounded by the small sizes of the fluid inclusions (typically <5 μm) and their salinity. This would lead to a bias in measured T_h (and thus mean T_h) toward vapor-bearing inclusions, which are likely to sit at the high end of what perhaps should be a normally distributed data population. This might explain the differences in the lower-temperature samples from basement veins at Navan, and possibly sample SPL070 (early Lisheen calcite; $T\Delta_{47}$ 48 ± 6°C; mean T_h 70°C), but not the sample from Birdhill (which is discussed below). In these cases, $T\Delta_{47}$ would be considered a true reflection of the primary temperature for the late calcite fill in these vein samples.

A final scenario is that the fluid inclusion populations in these samples are either more complex than realized (i.e., multiple fluid populations, zoned crystals), or they have been modified postentrapment due to thermal reequilibration or crystal deformation. In the latter case, fluid inclusions analyzed here showed no evidence for stretching and/or necking, leakage, or recrystallization and were analyzed along primary crystal growth zones. Instead, complex fluid inclusion populations might result in a mixed $T\Delta_{47}$ if more than one carbonate generation was drilled, or the T_h and $T\Delta_{47}$ analyses could be from noncontemporaneous carbonate phases. Honlet et al. (2018) discussed problems associated with differences in sample volumes for both techniques. Whereas T_h measurements can be obtained from individual crystals and growth zones, $T\Delta_{47}$ records an "averaged" temperature for the volume of material drilled. Multiple T_h analyses were obtained from three fluid inclusion chips by Everett (1999) from Birdhill basement vein sample BIR4. Whereas the first two yield very similar mean T_h values (181° and 172°C; range of two chips 157°–184°C), the last chip yielded a higher mean T_h of 218°C (range 180°–249°C, discounting two anomalously saline analyses) (Fig. 3).

This indicates that marked temperature variations occur across this vein sample, and thus our obtained $T\Delta_{47}$ value of 155° ± 14°C was most likely averaged from the lower-temperature material. In their study of the Peak District MVT province, Dennis et al. (2019) recorded episodic vein growth and $T\Delta_{47}$ between 40° and 100°C across 80-mm transects.

To summarize, the T_h and $T\Delta_{47}$ discrepancy from late calcite fills in Navan basement veins could reflect either the perturbation of the clumped isotope thermometer due to solid-state reordering or, perhaps more likely, the failure of vapor bubbles to nucleate in low-temperature (<80°C) fluid inclusions. In contrast, the discrepancy noted in the Birdhill vein sample is interpreted to be due to large natural temperature variations during dynamic vein growth at the crystal scale, with the clumped isotope analysis likely sampling lower-temperature calcite generations.

Applications and challenges to other deposit types

Clumped isotope thermometry has the potential to significantly advance our understanding of a number of mineral systems. Multiple fluid pulses can be recorded from individual samples at the mm to cm scale to help constrain the detailed fluid history of individual deposits (e.g., Figs. 2c-d; Dennis et al., 2019). The ability to obtain temperatures in the distal parts of ore systems, in deposit types where fluid inclusions may be lacking (e.g., sediment-hosted deposits; Sangster, 2018), or where fine-grained carbonate phases dominate, would be invaluable. When combined with traditional methods (e.g., salinity, δD, crush leach), novel in situ U-Pb carbonate geochronometry (e.g., Mangenot et al., 2018b) and/or fluid inclusion laser ablation-inductively coupled plasma-mass spectrometry (LA-ICP-MS) analysis (Wilkinson et al., 2009), additional insights could be gained. For example, MacDonald et al. (2019) recently applied both clumped C-O isotope thermometry and LA-ICP-MS U-Pb dating of calcite to basalt-hosted, low-temperature hydrothermal veins (75°–115°C) from three locations in Scotland. Through this approach, coupled with thermal modeling, the authors demonstrated that no closed-system resetting had occurred in at least two (likely all three) of the analyzed sites. Spatial and temporal Δ_{47} variations may also be combined with 3-D modeling to provide snapshots of developing mineral systems and may help as a vector to ore. However, all such studies must rely on a detailed paragenetic sequence of carbonates to extract the thermal and compositional history of the fluids.

Two significant challenges remain in applying clumped isotope thermometry to mineral systems: (1) the presence of fine-grained sulfides (and possibly high-salinity inclusions) resulting in erroneously high Δ_{48} and thus unreliable Δ_{47} values; and (2) resetting of $T\Delta_{47}$ during burial over geologic timescales. Regarding contamination, reliable data require meticulous sample screening and preparation. The introduction of small amounts of SO_2 gas into the mass spectrometer will produce $^{32}S^{16}O$ fragments, causing high Δ_{48} in subsequent samples (as in the case of our BMB analyses). A possible solution for samples containing very fine grained sulfides may lie in the development of clumped isotope methods based on infrared (IR) laser spectroscopy (e.g., Wang et al., 2020) or the cleaning of drilled carbonate powders to remove sulfides before digestion.

The problem of burial and/or subsequent orogenesis on $T\Delta_{47}$ is a concern for carbonates with low blocking temperatures, such as calcite; for hydrothermal deposits formed at 200° to 300°C (e.g., volcanogenic massive sulfide, Irish-type Zn-Pb, sedimentary-exhalative, Carlin-type); and perhaps dolomite, if these carbonates become subjected to elevated temperatures for extended periods of time. Δ_{47} from calcite and dolomite is unlikely to yield primary temperatures in deeply buried or long-lived basins (e.g., unconformity related uranium deposits, stratiform Cu) or from deposits preserved in orogenic belts (e.g., mesothermal gold; Carlin-type; see Quesnel et al., 2022) and metamorphosed VMS deposits. On the other hand, deposits containing both dolomite and calcite may present opportunities to constrain burial histories. Quesnel et al. (2022) argued that magnesite might be a more useful carbonate phase to retrieve original hydrothermal crystallization temperatures due to its suggested higher blocking temperatures (~490°C), though clumped C-O analysis of magnesite is not without its analytical challenges.

Conclusions

Clumped C-O isotope analysis represents a novel technique for determining hydrothermal carbonate precipitation temperatures and allows calculation of fluid $\delta^{18}O$ values in isotopic equilibrium with the measured carbonate. We demonstrate a close match between clumped isotope temperature ($T\Delta_{47}$) and fluid inclusion homogenization temperatures (T_h) from the Irish ore field. New insights into fluid-rock interaction processes at Lisheen include recognition of hydrothermal dolomitization at ~150° to 210°C, which led to the open-system recrystallization and isotopic resetting of early, fine-grained diagenetic dolomite. Subsequent carbonate phases were precipitated from hydrothermal fluids in isotopic equilibrium with these precursor, widespread dolomite phases, as ascending, ~170° to 220°C, mildly acidic fluids led to the development of BMB pseudobreccias in the Waulsortian. In the hanging wall of the Lisheen deposit, white hydrothermal dolomites formed at ~100° to 170°C, cementing subsidence breccias formed above the BMBs and orebodies. Clumped isotope analysis has the potential to significantly advance our understanding of a range of ore systems, particularly when combined with traditional methodologies (e.g., δD, crush-leach), and in situ techniques such as LA-ICP-MS and U-Pb carbonate geochronology. Perhaps the most significant hurdles to be overcome are a means to permit accurate analysis of samples containing fine-grained sulfides (present in many ore-stage carbonates) and isotopic resetting in long-lived basins and orogenic belts.

Acknowledgments

REFERENCES

Affek, H.P., 2012, Clumped isotope paleothermometry: Principles, applications, and challenges: The Paleontological Society Papers, v. 18, p. 101–114.

Allan, J.R., Beaty, D.W., Sturtevant, R.G., Hitzman, M.W., and Shearley, E., 1992, The origin of regional dolomite in the Waulsortian of Southeast Ireland: Implications for the time of ore deposition: Geological Society of America, Abstracts with Programmes, v. 24, A-354.

Anderson, I.K., Ashton, J.H., Boyce, A.J., Fallick, A.E., and Russell, M.J., 1998, Ore depositional processes in the Navan Zn-Pb deposit, Ireland: Economic Geology, v. 93, p. 535–563.

Anderson, N.T., Kelson, J.R., Kele, S., Daëron, M., Bonifacie, M., Horita, J., et al., 2021, A unified clumped isotope thermometer calibration (0.5-1100°C) using carbonate-based standardization: Geophysical Research Letters, v. 48, article e2020GL092069.

Andrew, C.J., 1986, The tectono-stratigraphic controls to mineralization in the Silvermines area, County Tipperary, Ireland, in Andrew, C.J., Crowe, R.W.A., Finlay, S., Pennell, W.M., and Pyne, J.F., eds., Geology and genesis of mineral deposits in Ireland: Dublin, Irish Association for Economic Geology, p. 377–418.

——2023, Irish Zn-Pb deposits—a review of the evidence for the timing of mineralization. Constraints of stratigraphy and basin development, in Andrew, C.J., Hitzman, M.W., and Stanley, G., eds., Irish-type Deposits around the world: Dublin, Irish Association for Economic Geology, p. 169–210, doi: 10.61153/CHFK3844.

Andrew, C.J., and Poustie, A., 1986, Syndiagenetic or epigenetic mineralization—the evidence from the Tatestown zinc-lead prospect, Co. Meath, in Andrew, C.J., Crowe, R.W.A., Finlay, S., Pennell, W.M., and Pyne, J.F., eds., Geology and genesis of mineral deposits in Ireland: Dublin, Irish Association for Economic Geology, p. 281–296.

Ashton, J.H., Blakeman, R., Geraghty, J., Beach, A., Coller, D., Philcox, M., Boyce, A., and Wilkinson, J.J., 2015, The giant Navan carbonate-hosted Zn-Pb deposit—a review, in Archibald, S.M., and Piercey, S.J., eds., Current perspectives on zinc deposits: Dublin, Irish Association for Economic Geology, p. 85–122.

Bergmann, K.D., Finnegan, S., Creel, R., Eiler, J.M., Hughes, N.C., Popov, L.E., and Fisher, W.W., 2018, A paired apatite and calcite clumped isotope thermometry approach to estimating Cambro-Ordovician seawater temperatures and isotopic composition: Geochimica et Cosmochimica Acta, v. 224, p. 18–41.

Bernasconi, S.M., Daëron, M., Bergmann, K.D., Bonifacie, M., Meckler, A.N., Affek, H.P., et al., 2021, InterCarb: A community effort to improve interlaboratory standardization of the carbonate clumped isotope thermometer using carbonate standards: Geochemistry, Geophysics, Geosystems, v. 22, article e2020GC009588.

Blakeman, R.J., Ashton, J.H., Boyce, A.J., Fallick, A.E., and Russell, M.J., 2002, Timing of interplay between hydrothermal and subsurface fluids in the Navan Zn + Pb orebody, Ireland: Evidence from metal distribution trends, mineral textures, and δ34S analyses: Economic Geology, v. 97, p. 73–91.

Bonifacie, M., Calmels, D., Eiler, J.M., Horita, J., Chaduteau, C., Vasconcelos, C., Agrinier, P., Katz, A., Passey, B.H., Ferry, J.F., and Bourrand, J.-J., 2017, Calibration of the dolomite clumped isotope thermometer from 25 to 350°C, and implications for a universal calibration for all (Ca, Mg, Fe)CO3 carbonates: Geochimica et Cosmochimica Acta, v. 200, p. 255–279.

Boyce, A.J., Anderton, R., and Russell, M.J., 1983, Rapid subsidence and early Carboniferous base-metal mineralization in Ireland: Transactions of the Institution of Mining and Metallurgy, v. 92, B55–66.

Braithwaite, C.J.R., and Rizzi, G., 1997, The geometry and petrogenesis of hydrothermal dolomites at Navan, Ireland: Sedimentology, v. 44, p. 421–440.

Came, R.E., Azmy, K., Tripati, A., and Olanipekun, B.-J., 2017, Comparison of clumped isotope signatures of dolomite cements to fluid inclusion thermometry in the temperature range of 73-176°C: Geochimica et Cosmochimica Acta, v. 199, p. 31–47.

Chang, B., Li, C., Liu, D., Foster, I., Tripati, A., et al., 2020, Massive formation of early diagenetic dolomite in the Ediacaran ocean: Constraints on the "dolomite problem": Proceedings of the National Academy of Sciences (PNAS), v. 117, p. 14005–14014.

Dennis, K.J., and Schrag, D.P., 2010, Clumped isotope thermometry of carbonatites as an indicator of diagenetic alteration: Geochimica et Cosmochimica Acta, v. 74, p. 4110–4122.

Dennis, K.J., Affek, H.P., Passey, B.H., Schrag, D.P., and Eiler, J.M., 2011, Defining an absolute reference frame for 'clumped' isotope studies of CO_2: Geochimica et Cosmochimica Acta, v. 75, p. 7117–7131.

Dennis, P.F., Myhill, D.J., Marca, A., and Kirk, R., 2019, Clumped isotope evidence for episodic, rapid flow of fluids in a mineralized fault system in the Peak District, UK: Journal of the Geological Society, London, v. 176, p. 447–461.

Dickson, J.A.D., Hodell, D.A., Swart, P.K., Lu, C., Mleneck-Vautravers, M.J., and Rolfe, J.E., 2023, Clumped isotope analysis of zoned calcite cement, Carboniferous, Isle of Man: The Depositional Record, doi: 10.1002/dep2.220.

Doran, A.L., 2021, Geochemical investigations of mineralising processes in the southern Irish Zn-Pb orefield: The combined application of isotope (S, clumped O-C, Sr, H) and mineral chemistry studies to track fluid flow: Ph.D. thesis, Dublin, University College Dublin, 300 p.

Doran, A.L., Hollis, S.P., Menuge, J.F., Piercey, S.J., Boyce, A.J., Johnson, S., Guven, J., and Turner O., 2022, A distal, high-grade Irish-type orebody: Petrographic, sulphur isotope, and sulphide chemistry of the Island Pod Zn-Pb orebody, Lisheen, Ireland: Economic Geology, v. 117, p. 305–326.

Doyle, E., and Bowden, A., 1995, Field guide to the Galmoy zinc-lead deposits, Co. Kilkenny, in Anderson, K., Ashton, J., Earls, G., Hitzman, M., and Tear, S., eds., Irish carbonate-hosted Zn-Pb deposits: Dublin, Irish Association for Economic Geology, p. 139-145.

Doyle, E., Bowden, A.A., Jones, G.V., and Stanley, G.A., 1992, The geology of the Galmoy zinc-lead deposits, Co. Kilkenny, in Bowden, A.A., Earls, G., O'Connor, P.G., and Pyne, J.F., eds., The Irish minerals industry 1980–1990: Dublin, Irish Association for Economic Geology, p. 211–225.

Drummond, D.A., 2021, Tara Deep zinc-lead deposit in Navan, Co. Meath, Ireland: Ore and carbonate depositional processes: Ph.D. thesis, University of Glasgow, 271 p., theses.gla.ac.uk/82454/.

Eiler, J.M., 2007, "Clumped-isotope" geochemistry—the study of naturally-occurring multiply-substituted isotopologues: Earth and Planetary Science Letters, v. 262, p. 309–327.

Eiler, J.M., and Schauble, E., 2004, $^{13}C^{18}O^{16}O$ in Earth's atmosphere: Geochimica et Cosmochimica Acta, v. 68, p. 4767–4777.

Everett, C.E., 1999, Tracing ancient fluid flow pathways: A study of the Lower Carboniferous base metal orefield in Ireland: Ph.D. thesis, New Haven, Connecticut, Yale University, 354 p.

Everett C.E., Wilkinson, J.J., and Rye, D.M., 1999a, Fracture-controlled fluid flow in the Lower Palaeozoic basement rocks of Ireland: Implications for the genesis of Irish-type Zn-Pb deposits, in McCaffrey, K.J.W., Lonergan, L., and Wilkinson, J.J., eds., Fractures, fluid flow and mineralization: Geological Society, London, Special Publications, v. 155, p. 247–276.

Everett, C.E., Rye, D.M., Wilkinson, J.J., Boyce, A.J., Ellam, R.M., Fallick, A.E., and Gleeson, S.A., 1999b, The genesis of Irish-type Zn-Pb deposits: Characterisation and origin of the principal ore fluid, in Stanley et al., eds., Mineral deposits: Processes to processing: Balkema, Rotterdam, p. 845–848.

Everett, C.E., Rye, D.M., and Ellam, R.M., 2003, Source or sink? An assessment of the role of the old red sandstone in the genesis of the Irish Zn-Pb deposits: Economic Geology, v. 98, p. 31–50.

Eyre, S.L., 1998, Geochemistry of dolomitization and Zn-Pb mineralization in the Rathdowney Trend, Ireland: Ph.D. thesis, University of London, 414 p.

Friedman, I., and O'Neil, J.R., 1977, Compilation of stable isotope fractionation factors of geochemical interest: United States Geological Survey, Professional Paper 440. doi: 10.1017/CBO9781107415324.004.

Fusciardi, L.P., Guven, J.F., Stewart, D.R.A., Carboni, V., and Walsh, J.J., 2003, The geology and genesis of the Lisheen Zn-Pb deposit, Co. Tipperary, Ireland, in Kelly, J.G., Andrew, C.J., Ashton, J.H., Boland, M.B., Earls, G., Fusciardi, L., and Stanley, G., eds., Europe's major base metal deposits: Dublin, Irish Association for Economic Geology, p. 455–481.

Ghosh, P., Adkins, J., Affek, H., Balta, B., Guo, W., Schauble, E. A., et al., 2006, ^{13}C–^{18}O bonds in carbonate minerals: A new kind of paleothermometer: Geochimica et Cosmochimica Acta, v. 70, p. 1439–1456.

Gregg, J.M., Shelton, K.L., Johnson, A.W., Somerville, I.D., and Wright, W.R., 2001, Dolomitization of the Waulsortian Limestone (Lower Carboniferous) in the Irish Midlands: Sedimentology, v. 48, p. 645–766.

Guo, W., Mosenfelder, J.L., Goddard, I.I.I., William, A., and Eiler, J.M., 2009, Isotopic fractionations associated with phosphoric acid digestion of carbonate minerals: Insights from first-principles theoretical modeling and clumped isotope measurements: Geochimica et Cosmochimica Acta, v. 73, p. 7203–7225.

Hitzman, M.W., 1986, Geology of the Abbeytown mine, Co. Sligo, Ireland, in Andrew, C.J., Crowe, R.W.A., Finlay, S., Pennell, W.M., and Pyne, J.F., eds., Geology and genesis of mineral deposits in Ireland: Dublin, Irish Association for Economic Geology, p. 341–354.

Hitzman, M.W., and Beaty, D.W., 1996, The Irish Zn-Pb-(Ba) orefield: Society of Economic Geologists, Special Publication no. 4, p. 112–143.

Hitzman, M.W., O'Connor, P., Shearley, E., Schaffalitzky, C., Beaty, D.W., Allan, J.R., and Thompson, T.B., 1992, Discovery and geology of the Lisheen Zn-Pb-Ag prospect, Rathdowney Trend, Ireland, in Bowden, A.A., Earls, G., O'Connor, P.G., and Pyne, J.F., eds., The Irish mineral industry: Dublin, Irish Association for Economic Geology, p. 227–246.

Hitzman, M.W., Allan, J.R., and Beaty, D.W., 1998, Regional dolomitization of the Waulsortian limestone in southeastern Ireland: Evidence of large-scale fluid flow driven by the Hercynian orogeny: Geology, v. 26, p. 547–550.

Hitzman, M.W., Redmond, P.B., and Beaty, D.W., 2002, The carbonate-hosted Lisheen Zn-Pb-Ag deposit, County Tipperary, Ireland: Economic Geology, v. 97, p. 1627–1655.

Honlet, R., Gasparrini, M., Muchez, P., Swennen, R., and John, C.M., 2018, A new approach to geobarometry by combining fluid inclusion and clumped isotope thermometry in hydrothermal carbonates: Terra Nova, v. 30, p. 199–206.

Horita, J., 2014, Oxygen and carbon isotope fractionation in the system dolomite-water-CO_2 to elevated temperatures: Geochimica et Cosmochimica Acta, v. 129, p. 111–124.

Hu, X., Müller, I.A., Zhao, A., Ziegler, M., Chen, Q., et al., 2022, Clumped isotope thermometry reveals diagenetic origin of the dolomite layer within late Ordovician black shale of the Guanyinqiao bed (SW China): Chemical Geology, v. 588, article 120641.

John, C.M., 2018, Burial estimates constrained by clumped isotope thermometry: example of the Lower Cretaceous Quishn Formation (Haushi-Huqf High, Oman): Geological Society, London, Special Publication 435, p. 107–121.

Kim, S.-T., and O'Neil, J.R., 1997, Equilibrium and nonequilibrium oxygen isotope effects in synthetic carbonates: Geochimica et Cosmochimica Acta, v. 61, p. 3461–3475.

Kirk, R., 2017, Development of clumped isotope techniques and their application to palaeoclimate studies: Unpub. Ph.D. thesis, Norwich, United Kingdom, University of East Anglia, 218 p.

Kluge, T., John, C.M., Jourdan, A.-L., Davis, S., and Crawshaw, J., 2015, Laboratory calibration of the calcium carbonate clumped isotope thermometer in the 25-250°C temperature range: Geochimica et Cosmochimica Acta, v. 157, p. 213–227.

Konari, M.B., and Rastad, E., 2018, Nature and origin of dolomitization associated with sulphide mineralization: New insights from the Tappehsorkh Zn-Pb(-Ag-Ba) deposit, Irankuh mining district, Iran: Geological Journal, v. 53, p. 1–21.

Kyne, R., Torremans, K., Güven, J., Doyle, R., and Walsh, J., 2019, 3-D modeling of the Lisheen and Silvermines deposits, County Tipperary, Ireland: Insights into structural controls on the formation of Irish Zn-Pb deposits: Economic Geology, v. 114, p. 93–116.

Lee, M.J., 2002, Origin and Zn-Pb mineralization of dolomite breccias in the Irish Midlands: Unpub. Ph.D. thesis, Imperial College, University of London, 256 p.

Lloyd, M.K., Eiler, J.M., and Nabelek, P.I., 2017, Clumped isotope thermometry of calcite and dolomite in a contact metamorphic environment: Geochimica et Cosmochimica Acta, v. 197, p. 323–344.

Lloyd, M.K., Ryb, U., and Eiler, J.M., 2018, Experimental calibration of clumped isotope reordering in dolomite: Geochimica et Cosmochimica Acta, v. 242, p. 1–20.

MacDonald, J.M., John, C.M., and Girard, J.-P., 2018, Testing clumped isotopes as a reservoir characterization tool: A comparison with fluid inclusions in a dolomitized sedimentary carbonate reservoir buried to 2–4 km: Geological Society, London, Special Publication 468, p. 189–202.

MacDonald, J.M., Faithfull, J.W., Roberts, N.M.W., Davies, A.J., Holdsworth, C.M., Newton, M., Boyce, A.J., and John, C.M., 2019, Clumped-isotope

palaeothermometry and LA-ICP-MS U-Pb dating of lava-pile hydrothermal calcite veins: Contributions to Mineralogy and Petrology, v. 174, article 63.

Mangenot, X., Gasparrini, M., Rouchon, V., and Bonifacie, M., 2018a, Basin-scale thermal and flow histories revealed by carbonate clumped isotopes (Δ47)—Middle Jurassic carbonates of the Paris basin depocenter: Sedimentology, v. 65, p. 123–150.

Mangenot, X., Gasparrini, M., Gerdes, A., Rouchon, V., and Bonifacie, M., 2018b, An emerging thermochronometer for carbonate-bearing rocks: Δ47/(U-Pb): Geology, v. 46, p. 1067–1070.

Marks, F.R., 2015, Remote detection of Irish-type orebodies: An investigation of the Navan halo: Ph.D. thesis, Dublin, University College Dublin, 226 p.

Menuge, J.F., Daly, J.S., and Walshaw, J.D., 2007, Formation of Irish-type base metal deposits by multiple deep hydrothermal convection cells: Evidence from a regional fluid inclusion and Sr-Nd isotope study, in Andrew, C.J., et al., eds., Digging deeper: Proceedings of the 9th Biennial SGA Meeting, Dublin: SGA, p. 291–294.

Mering, J.A., Barker, S.L.L., Huntington, K.W., Simmons, S., Dipple, G., Andrew, B., and Schauer, A., 2018, Taking the temperature of hydrothermal ore deposits using clumped isotope thermometry: Economic Geology, v. 113, p. 1671–1678.

Petersen, S.V., Winkelstern, I.Z., Lohmann, K.C., and Meyer, K.W., 2016, The effects of Porapak™ trap temperature on δ18O, δ13C, and Δ47 values in preparing samples for clumped isotope analysis: Rapid Communications in Mass Spectrometry, v. 30, p. 199–208.

Petersen, S.V., Defliese, W.F., Saenger, C., Daërons, M., Huntington, K.W., John, C.M., et al., 2019, Effects of improved 17O correction on interlaboratory agreement in clumped isotope calibrations, estimates of mineral specific offsets, and temperature dependence of acid digestion fractionation: Geochemistry, Geophysics, Geosystems, v. 20, p. 3495–3519, doi: 10.1029/2018GC008127.

Philcox, M.E., 1984, Lower Carboniferous litho-stratigraphy of the Irish Midlands: Special Publication, Irish Association for Economic Geology, Dublin, 89 p., https://www.gsi.ie/en-ie/publications/Pages/Lower-Carboniferous-Stratigraphy-of-the-Irish-Midlands-M-E-Philcox-1984.aspx..

Quesnel, B., Jautzy, J., Scheffer, C., Raymond, G., Beaudoin, G., Jørgensen, T.R.C., and Pinet, N., 2022, Clumped isotope geothermometry in Archean mesothermal hydrothermal systems (Augmitto-Bouzan orogenic gold deposit, Abitibi, Quebec, Canada): A note of caution and a look forward: Chemical Geology, v. 610, article 121099.

Rosenbaum, J., and Sheppard, S.M.F., 1986, An isotopic study of siderites, dolomites and ankerites at high temperatures: Geochimica et Cosmochimica Acta, v. 50, p. 1147–1150.

Samson, I.M., and Russell, M.J., 1987, Genesis of the Silvermines zinc-lead-barite deposit, Ireland: Fluid inclusion and stable isotope evidence: Economic Geology, v. 82, p. 371–394.

Sangster, D.F., 2018, Toward an integrated genetic model for vent-distal SEDEX deposits: Mineralium Deposita, v. 53, p. 509–527.

Shearley, E., Redmond, P., Goodman, R., and King, M., 1995, A guide to the Lisheen Zn-Pb deposit: Society of Economic Geologists, Guidebook Series, v. 21, p. 123–137.

Singer, S.B., 1995, World class base and precious metal deposits—a quantitative analysis: Economic Geology, v. 90, p. 88–104.

Swart, P.K., Burns, S.J., and Leder, J.J., 1991, Fractionation of the stable isotopes of oxygen and carbon in carbon dioxide during the reaction of calcite with phosphoric acid as a function of temperature and technique: Chemical Geology (Isotope Geoscience Section), v. 86, p. 89–96.

Torremans, K., Kyne, R., Doyle, R., Guven, J.F., and Walsh, J.J., 2018, Controls on metal distributions at the Lisheen and Silvermines deposits: Insights into fluid flow pathways in Irish-type Zn-Pb deposits: Economic Geology, v. 113, p. 1455–1477.

Turner, O., Hollis, S., Guven, J., and McClenaghan, S., 2019, Establishing a geochemical baseline for the Lower Carboniferous stratigraphy of the Rathdowney Trend, Irish Zn-Pb orefield: Journal of Geochemical Exploration, v. 196, p. 259–269.

Veizer, J., Ala, D., Azmy, K., Bruckschen, P., Buhl, D., Bruhn, F., Carden, G.A.F., Diener, A., Ebneth, S., Godderis, Y., Jasper, T., Korte, C., Pawellek, F., Podlaha, O.G., and Strauss, H., 1999, 87Sr/86Sr, δ13C and δ18O evolution of Phanerozoic seawater: Chemical Geology, v. 161, p. 59–88.

Walshaw, R.D., Menuge, J.F., and Tyrrell, S., 2006, Metal sources of the Navan carbonate-hosted base metal deposit, Ireland: Nd and Sr isotope evidence for deep hydrothermal convection: Mineralium Deposita, v. 41, p. 803–819.

Wang, Z., Schauble, E.A., and Eiler, J.M., 2004, Equilibrium thermodynamics of multiply substituted isotopologues of molecular gases: Geochimica et Cosmochimica Acta, v. 68, p. 4779–4797.

Wang, Z., Nelson, D.D., Dettman, D.L., McManus, J.B., Quade, J., Huntington, K.W., Schauer, A.J., and Sakai, S., 2020, Rapid and precise analysis of carbon dioxide clumped isotopic composition by tunable infrared laser differential spectroscopy: Analytical Chemistry, v. 92, p. 2034–2042.

Wilkinson, J.J., 2001, Fluid inclusions in hydrothermal ore deposits: Lithos, v. 55, p. 229–272.

——2003, On diagenesis, dolomitisation and mineralisation in the Irish Zn-Pb orefield: Mineralium Deposita, v. 38, p. 968–983.

——2010, A review of fluid inclusion constraints on mineralization in the Irish ore field and implications for the genesis of sediment-hosted Zn-Pb deposits: Economic Geology, v. 105, p. 417–442.

——2014, Sediment-hosted zinc-lead deposits: Processes and perspectives, in Holland, H.D., and Turekian, K.K., eds., Treatise on geochemistry, 2nd ed.: Oxford, Elsevier, p. 219–249.

——2017, Metastable freezing: A new method for the estimation of salinity in aqueous fluid inclusions: Economic Geology, v. 112, p. 185–193.

Wilkinson, J.J., and Earls, G., 2000, A high-temperature hydrothermal origin for black dolomite matrix breccias in the Irish Zn-Pb orefield: Mineralogical Magazine, v. 64, p. 1017–1036.

Wilkinson, J.J., and Hitzman, M.W., 2015, The Irish Zn-Pb orefield: The view from 2014, in Archibald, S.M., and Piercey, S.J., eds., Current perspectives on zinc deposits: Dublin, Irish Association for Economic Geology, p. 59–72.

Wilkinson, J.J., Everett, C.E., Boyce, A.J., Gleeson, S.A., and Rye, D.M., 2005a, Intracratonic crustal seawater circulation and the genesis of subseafloor zinc-lead mineralization in the Irish orefield: Geology, v. 33, p. 805–808.

Wilkinson, J.J., Eyre, S.L., and Boyce, A.J., 2005b, Ore-forming processes in Irish-type carbonate-hosted Zn-Pb deposits: Evidence from mineralogy, chemistry and isotopic composition of sulfides at the Lisheen mine: Economic Geology, v. 100, p. 63–86.

Wilkinson, J.J., Stoffell, B., Wilkinson, C.C., Jeffries, T.E., and Appold, M.S., 2009, Anomalously metal-rich fluids form hydrothermal ore deposits: Science, v. 323, p. 764–767.

Wilkinson, J.J., Crowther, H.L., and Coles, B.J., 2011, Chemical mass transfer during hydrothermal alteration of carbonates: Controls of seafloor subsidence, sedimentation and Zn-Pb mineralization in the Irish Carboniferous: Chemical Geology, v. 289, p. 55–75.

Yapparova, A., Gabellone, T., Whitaker, F., Kulik, D.A., and Matthai, S.K., 2017, Reactive transport modelling of hydrothermal dolomitisation using the CSMP++GEM coupled code: Effects of temperature and geological heterogeneity: Chemical Geology, v. 466, p. 562–574.

Yesares, L., Drummond, D.A., Hollis, S.P., Doran, A.L., Menuge, J.F., Boyce, A.J., Blakeman, R.J., and Ashton, J.H., 2019, Coupling mineralogy, texture, stable and radiogenic isotopes in identifying ore-forming processes in Irish-type carbonate-hosted Zn-Pb deposits: Minerals, v. 9, article 335, doi: 10.3390/min9060335.

Steven Hollis is a lecturer in ore systems at the University of Edinburgh. He obtained his undergraduate degree from the University of Birmingham in 2007, his M.Sc. in geochemistry from the University of Leeds in 2008, and his Ph.D. from the University of Southampton in 2013. Subsequent postdoctoral research focused on Archaean VMS mineralization in Western Australia and the applications of clumped C-O and Pb isotope systems to the Irish Zn-Pb ore field. He is currently researching the applications of mineral chemical and isotope geochemistry to constrain ore-forming processes and aid exploration for VMS, sediment-hosted, and orogenic gold systems.